

PHYSICAL REVIEW LETTERS

VOLUME 26

8 MARCH 1971

NUMBER 10

Experiments on the Relation Between Radiation and Fluctuation Spectrum of a Turbulent Plasma*

L. D. Bollinger and H. Böhmer

Department of Physics and Coordinated Science Laboratory, University of Illinois, Urbana, Illinois 61801

(Received 21 December 1970)

The experimentally observed radiation from unstable plasma waves generated by the interaction of an electron beam with a plasma is compared with the longitudinal fluctuation spectrum, determined by incoherent microwave scattering. The results are in agreement with a theory by Ichimaru and Starr for the electromagnetic radiation from anisotropic turbulent plasmas.

The conversion of longitudinal plasma waves to transverse waves has become an important phenomenon for laboratory plasmas and plasmas of astrophysical origin because, in principle, the received radiation permits one to obtain information about the collective plasma behavior. Several mechanisms for the process have been proposed in the past.¹⁻⁷

Recently, Ichimaru and Starr⁸ proposed a simple model for radiation from a turbulent anisotropic plasma based on the fact that in the dispersion relation the longitudinal part cannot be uncoupled from the transverse part. The anisotropy may be caused by a particle stream or a magnetic field. The transverse part of these quasi-longitudinal waves can propagate out of the plasma and subsequently be observed as radiation. Consequently, the frequency and direction of propagation of radiation are the same as those of the plasma waves from which they were emitted and the radiated power is determined by the dynamic form factor for the plasma fluctuations, $S(\vec{k}, \omega)$. \vec{k} and ω are the plasma-wave wave number and frequency.

In this experiment we simultaneously measure the radiation and the incoherent microwave scattering from longitudinal electron-plasma waves generated by an electron beam passing through a plasma (Fig. 1). The microwave scattering gives

a direct measure of $S(\vec{k}, \omega)$.⁹ \vec{k} and ω are determined by $\vec{k} = \vec{k}_s - \vec{k}_i$ and $\omega = \omega_s - \omega_i$, and \vec{k}_s and \vec{k}_i are the scattered- and incident-microwave wave numbers, and ω_s and ω_i the scattered- and incident-microwave frequencies. By varying the directions of the microwaves incident on and the scattered microwaves received from the plasma, plasma waves of different magnitudes of \vec{k} and different directions θ of propagation relative to the beam axis can be selected. In the experiment we select for each direction θ the most unstable plasma wave whose frequency ω_{opt} and wave number k_{opt} are given by $\omega_{opt} \simeq \omega_p$, $k_{opt} \simeq \omega_p /$

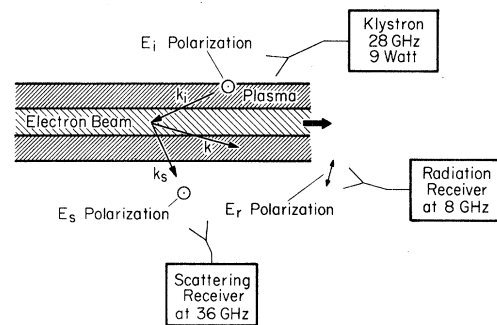


FIG. 1. Schematic for simultaneous measurement of radiation and microwave scattering. \vec{k}_i and \vec{k}_s are the incident- and scattered-microwave numbers, and \vec{k} the plasma-wave wave number. \vec{E}_i , \vec{E}_s , and \vec{E}_r are the electric-field vectors of the incident, scattered, and radiated microwaves.

$v_0 \cos \theta$.¹⁰ $\omega_p = (4\pi n e^2 / m)^{1/2}$, n = electron plasma density, and v_0 = electron beam velocity.

The incident microwaves are focused onto and the scattered microwaves received from the plasma by means of dielectric-lens corrected horns of 3° angular resolution. The radiation receiving horn is a dielectric-rod horn combination with 5° angular resolution. The scattering horn system and the radiation horn can be moved along the axis of the beam to look at different stages of the spatial plasma-wave development.

The plasma is the afterglow of a low-pressure discharge in neon, having a decay time constant of about 200 μ sec and a repetition frequency of 15 Hz. The electron beam, with 20 keV energy, current variable up to 1 A, 1 cm diam, and a duration of 2 μ sec, can be exposed to effectively constant plasma densities of 10^{13} to 10^{10} cm⁻³. The plasma densities are determined with a microwave interferometer. Additional ionization during the interaction of the beam with the plasma was found to be negligible under the experimental conditions considered here. There is no external magnetic field present in the plasma. The rectified outputs of the K_u -band scattering receiver and the X-band radiation receiver are each detected by separate lock-in amplifiers synchronized to the 15-Hz reference frequency.

To investigate the relation between the direction of propagation of the longitudinal plasma waves and the direction of the emitted radiation, we make use of the plasma-wave intensity being strongly peaked for wave numbers in the direction of 35–40° to the beam axis in the initial stage of the plasma-wave development, a finite-beam effect. We find that the radiation intensity is strongly peaked in the same direction (Fig. 2).

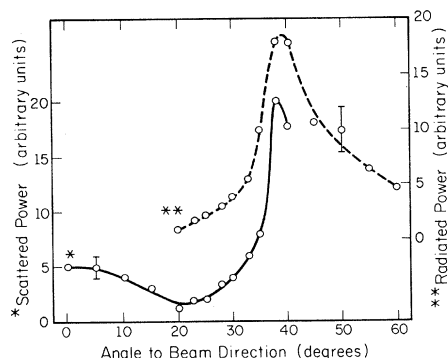


FIG. 2. Microwave power scattered and power radiated from plasma waves propagating at various angles θ with respect to the beam direction. Observation of scattering is experimentally limited to $\theta < 40^\circ$ and radiation to $\theta > 20^\circ$. Electron-beam current = 250 mA.

In our measurements the radiation frequency is the same as the plasma-wave frequency, determined by scattering, within the experimental accuracy of 1%. The emitted radiation is strongly polarized parallel to the plane given by \vec{k} and \vec{v}_0 . These observations confirm the frequency, direction of propagation, and polarization of the radiation predicted by Ichimaru and Starr.

To evaluate the radiation process quantitatively, we experimentally measure the ratio of the power radiated at an angle θ to the beam axis per unit solid angle to the power scattered from plasma waves propagating at the same angle θ per unit solid angle. The corresponding ratio, predicted by the Ichimaru-Starr theory,⁸ is

$$\frac{dP_r/d\Omega_r}{dP_s/d\Omega_s} = \frac{k_b^4 m_e v_0^2}{2\pi^2 r_0 l} \omega_0 \times \sin^2 \theta \int_0^\infty dk \frac{W(k)}{k^5} \frac{\Delta\omega_r}{\Delta\omega_s} \frac{A_n}{V_s}, \quad (1)$$

where $k_b^2 = 4\pi n_b e^2 / m_e (\Delta v)^2$, n_b = electron beam density, Δv = beam velocity spread, and l = incident microwave intensity = 1.0 W/cm². $W(k)$ is a normalized weighting function strongly peaked at k_{opt} which gives the shape of the k spectrum at the plasma-wave frequency ω_0 . $\Delta\omega_r/2\pi$ and $\Delta\omega_s/2\pi$ are the bandwidths of the radiation and scattering receivers, both equal to 8 MHz. A_n is defined by $A_n = \vec{A}_n \cdot \vec{k} / |\vec{k}|$, where \vec{A}_n is the beam-surface vector area seen by the radiation horn. V_s is the scattering volume.

Because of the lack of spatial resolution along the beam axis of the radiation receiving horn, comparison of Eq. (1) with the experiment was done in the saturation stage of the instability where the plasma-wave amplitude does not change rapidly in space (Fig. 3, curve *a*). Using a shape for $W(k)$ measured experimentally for $\theta = 0$, and assuming that its shape remains the same for other θ , we find for Eq. (1)

$$\frac{dP_r/d\Omega_r}{dP_s/d\Omega_s} = 1.1 \times 10^{-16} \frac{n_b^2}{(\Delta v/v_0)^4} \times \sin^2 \theta \cos^5 \theta \pm 30\%. \quad (2)$$

The error is mainly due to the uncertainty in the determination of the beam diameter. The factor $\cos^5 \theta$ reflects the θ dependence of k_{opt} .

This equation has three experimentally observable aspects: the absolute value of this ratio, the dependence on θ , and the dependence on the beam velocity spread Δv . A comparison of the angular dependence of this power ratio to the experimental data is inconclusive because of the

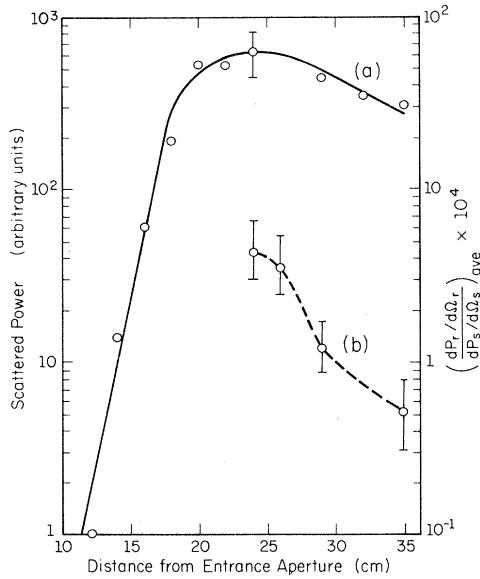


FIG. 3. Curve *a*: An example of on-axis spatial growth of the most unstable plasma waves ($\theta=0$). Curve *b*: Ratio of radiated to scattered power averaged over all observable angles at and beyond the saturation stage at the instability. Beam current = 440 mA.

experimental error. Also, good agreement may not be expected since the Ichimaru-Starr theory does not take into account the effects of the boundary on the emitted radiation for non-normal incidence, and because of our assumption of no angular dependence in the weighting function $W(k)$.

A good test of the validity of the Ichimaru-Starr theory should be a comparison of the experimental angle-averaged values for the radiated-to-scattered power ratios. This requires knowledge of the beam velocity spread which increases as the plasma-wave spectrum develops and cannot be measured directly.

To determine $\Delta v/v_0$ we make use of the Ascoli-Singhaus criterion¹¹ which predicts that in a regime where collisions dominate the growth rate, a warm beam-plasma system becomes stabilized if the relative beam velocity spread exceeds a value given by

$$(\Delta v/v_0)^2 = 0.66 \alpha \omega_p / \nu_c, \quad (3)$$

where α = ratio of the beam to plasma electron density and ν_c = effective plasma electron collision frequency. This relation has been verified by Böhmer, Chang, and Raether¹² who also showed that, for experimental conditions identical to those of Fig. 3, an initially cold beam acquires a relative velocity spread given by Eq. (3) at the point of maximum wave amplitude. Using the criterion (3) we find from Eq. (2), for the

conditions of Fig. 3,

$$\left. \frac{dP_r/d\Omega_r}{dP_s/d\Omega_s} \right|_{\text{calc. at max instability}} = (2.2 \pm 0.7) \times 10^4.$$

This predicted ratio compares favorably with the experimentally determined value at 26 cm (Fig. 3, curve *b*):

$$\left. \frac{dP_r/d\Omega_r}{dP_s/d\Omega_s} \right|_{\text{meas. at max instability}} = (3.6 \pm 2.5) \times 10^4.$$

In Ref. 12 it was found that the beam-velocity spread increases beyond the point of maximum instability. From Eq. (2) one should therefore expect a decrease in the radiated-to-scattered power ratio. This is in qualitative agreement with the results of Fig. 3 where the ratio decreased from 4.4×10^4 at 24 cm to 0.53×10^4 at 35 cm.

Our results indicate the radiation arising from the quasilongitudinal plasma-wave nature to be the dominant radiation mechanism, at least for the beam-plasma interaction. Other theories¹⁻⁷ do not require the emitted radiation to be in the same direction as the plasma-wave propagation. We conclude that radiation as a diagnostic tool for beam-plasma instability must take into account the decrease in radiation due to an increase in beam temperature. In general, for any anisotropic plasma the effect of parameters related to the anisotropy must be considered. Finally, it should be mentioned that the energy lost from the plasma by radiation is small. For example, in the experiment of Fig. 3 at 24 cm the power radiated at 30° to the beam direction is about $1.5 \times 10^{-2}\%$ of the plasma-wave power in the same direction.

We are thankful to Professor M. Raether for helpful advice and to Professor S. Ichimaru for informative discussions.

*Work supported by the Joint Services Electronics Program (U. S. Army, U. S. Navy and U. S. Air Force) under Contract No. DAAB-07-67-C-0199.

¹D. A. Tidman, Phys. Rev. **117**, 366 (1960).

²K. H. Dunphy, D. Kahn, and D. Mintzer, Phys. Fluids **10**, 162 (1967).

³T. H. Dupree, Phys. Fluids **7**, 923 (1964).

⁴D. A. Tidman and T. H. Dupree, Phys. Fluids **8**, 1860 (1965).

⁵T. Dawson and C. Oberman, Phys. Fluids **5**, 517 (1962).

⁶V. N. Tsytovich, Usp. Fiz. Nauk **90**, 435 (1966) [Sov.

Phys. Usp. **9**, 805 (1967)].

⁷S. A. Kaplan and V. N. Tsytovich, *Astron. Zh.* **44**, 1194 (1967) [*Sov. Phys. Astron.* **11**, 956 (1968)].

⁸S. Ichimaru and S. H. Starr, *Phys. Rev. A* **2**, 821 (1970). The radiation-to-scattering ratio of Ichimaru and Starr is adapted to include the finite receiver bandwidths, the radiating area, and the scattering volume, and uses a warm-beam approximation.

⁹M. N. Rosenbluth and N. Rostoker, *Phys. Fluids* **5**, 776 (1962); H. Böhmer and M. Raether, *Phys. Rev. Lett.* **16**, 1145 (1966).

¹⁰S. A. Bludman, K. M. Watson, and M. N. Rosenbluth, *Phys. Fluids* **3**, 747 (1960).

¹¹H. E. Singhaus, *Phys. Fluids* **7**, 1534 (1964).

¹²H. Böhmer, J. Chang, and M. Raether, *Phys. Fluids* **14**, 150 (1971).

Umklapp Optical Third-Harmonic Generation in Cholesteric Liquid Crystals

J. W. Shelton and Y. R. Shen

Department of Physics, University of California, Berkeley, California 94720, and Inorganic Materials Research Division, Lawrence Radiation Laboratory, Berkeley, California 94720

(Received 11 January 1971)

We have observed, in cholesteric liquid crystals, optical umklapp processes with which the third-harmonic generation is phase matched. We show that phase-matched third-harmonic generation can be used to measure both the width and the asymmetry of ultrashort pulses.

We have previously reported on the observation of optical third-harmonic generation in a cholesteric liquid crystal satisfying a certain phase-matching condition.¹ However, because of the unusual characteristics of cholesteric liquid crystals, there exist many different phase-matching conditions. In particular, some of them require simultaneous presence of fundamental waves propagating in opposite directions. In still other cases, the third harmonic emerges propagating backward with respect to the incoming fundamental. It is obvious that in these processes the total momentum of the interacting waves cannot be conserved; but, as will be shown later, the momentum mismatch here is actually compensated by the lattice momentum, which has a unit of $(4\pi/p)\hbar$ where p is the helical pitch of the cholesteric substance. In analogy to electrons propagating in a periodic lattice, we can describe such phase-matched third-harmonic generation processes as coherent optical umklapp processes, or nonlinear Bragg reflection.² In this paper, we would like to report on the observation of such processes. We also show that these processes provide a technique for mea-

surements of pulse width and pulse asymmetry.

Analysis of collinear phase matching of third-harmonic generation in a cholesteric liquid crystal along the helical axis (the z axis) has been given in Ref. 1. For the sake of clarity, we reproduce here the equations serving as definitions for the various quantities. According to de Vries,³ the two modes of linear wave propagation along \hat{z} , in the rotating coordinate system defined by $\hat{\xi} = \hat{x} \cos(2\pi z/p) + \hat{y} \sin(2\pi z/p)$, $\hat{\eta} = -\hat{x} \sin(2\pi z/p) + \hat{y} \cos(2\pi z/p)$, and $\hat{z}' = \hat{z}$, are

$$(E_T^{(\omega)})_{\pm} = (\mathcal{E}_{\xi} \hat{\xi} + \mathcal{E}_{\eta} \hat{\eta})_{\pm}^{(\omega)} \exp[ik_{\pm}^{(\omega)} z - i\omega t],$$

with

$$k_{\pm}^{(\omega)} = k_0^{(\omega)} m_{\pm}^{(\omega)},$$

$$(m_{\pm}^{(\omega)})^2 = (\lambda'^2 + 1) \pm (4\lambda'^2 + \alpha^2)^{1/2},$$

$$\left(\frac{\mathcal{E}_{\eta}}{\mathcal{E}_{\xi}}\right)_{\pm}^{(\omega)} \equiv if_{\pm}^{(\omega)} = \frac{i2m_{\pm}^{(\omega)}\lambda'}{m_{\pm}^2 + \lambda'^2 - (1 + \alpha)}, \quad (1)$$

where $k_0^{(\omega)} = \omega\epsilon^{1/2}/c$, $\lambda' = 2\pi c/\omega p\epsilon^{1/2}$, $\epsilon = (\epsilon_{\xi} + \epsilon_{\eta})/2$, $\alpha = (\epsilon_{\xi} - \epsilon_{\eta})/2\epsilon$, and ϵ_{ξ} and ϵ_{η} are the dielectric constants along $\hat{\xi}$ and $\hat{\eta}$. In the lab frame, the expression for the field becomes

$$\vec{E}_{\pm}^{(\omega)} = [(\hat{x} + i\hat{y})(1 + f_{\pm}^{(\omega)}) + (\hat{x} - i\hat{y})(1 - f_{\pm}^{(\omega)}) \exp(i4\pi z/p)](\mathcal{E}_{\xi}^{(\omega)}/2) \exp[i(k_{\pm}^{(\omega)} - 2\pi/p)z - i\omega t]. \quad (2)$$

Note that for $\lambda'^2 > \epsilon_{\xi}/\epsilon$, a negative $k_{-}^{(\omega)}$ corresponds to propagating waves with the Poynting vector in the $+\hat{z}$ direction, and vice versa.

If we allow waves to propagate in both $+\hat{z}$ and $-\hat{z}$ directions, then collinear phase matching of third-harmonic generation results when $[\pm k_{\pm}^{(\omega)} \pm k_{\pm}^{(\omega)} \pm k_{\pm}^{(\omega)}] - [\pm k_{\pm}^{(3\omega)}] = 0$ for any combination of signs in the expression.¹ This can be achieved by adjusting the helical pitch by external means such as changing the temperature of the sample. Although we have observed most of these different phase-matching